

Asymptotic Giant Branch Stars as Astroparticle Laboratories

Inma Domínguez,¹ Oscar Straniero,² and Jordi Isern³

¹*Depto. de Física Teórica y del Cosmos, Universidad de Granada, 18071 Granada, Spain (inma@ugr.es)*

²*Osservatorio Astronomico di Collurania, 64100 Teramo, Italy (straniero@astr.te.astro.it)*

³*Institut d'Estudis Espacials de Catalunya, IEEC/CSIC, Barcelona, Spain (isern@ieec.fcr.es)*

19 April 2018

ABSTRACT

We show that the inclusion of axion emission during stellar evolution introduces important changes into the evolutionary behaviour of AGB stars. The mass of the resulting C/O white dwarf is much lower than the equivalent obtained from standard evolution. This implies a deficit in luminous AGB stars and in massive WDs. Moreover the total mass processed in the nuclear burning shells that is dredged-up to the surface ($3^{\text{rd}}D_{up}$) increases when axion emission is included, modifying the chemical composition of the photosphere. We conclude that the AGB is a promising phase to put constraints on particle physics

Key words: Axions–Stellar Evolution–AGB–WD.

1 INTRODUCTION

It is well known that the standard theory does not predict several properties of the elementary particles (such as mass and magnetic moment). Furthermore, the different non-standard theories leave open the possibility that unknown (exotic) particles could still exist. In the recent past, several attempts have been made to understand how these particles could modify stellar evolution and, in turn, to use these modifications to constrain particle theory (see Raffelt 1996 for a recent review). The general procedure consists in the comparison of the observed properties of selected stars (or of a cluster of stars) with the prediction of theoretical stellar models obtained under different assumptions about the microphysics input.

Axions and WIMPS (Weak Interactive Massive Particles) are the most promising candidates for non baryonic dark matter. Non accelerator tests for axions in the acceptable mass range are up to date available. In this situation, stars in general and especially the best-known one, the Sun, are being widely used to test particle physics. Several experiments to detect solar and galactic axions have been performed (Sikivie 1983; Lazarus et al. 1992). Experiments with better sensitivity are currently underway (van Bibber et al. 1994; Hagmann et al. 1996 and 1998 (U.S. Axion Search); Matsuki et al. 1996 (Kyoto experiment CAR-RACK); Moriyama 1998, Moriyama et al. 1998; Avignone III et al. 1998 and Gattone et al. (SOLAX collaboration)) and there is a proposal to use the Large Hadron Collider at CERN (Zioutas et al. 1998) to detect solar axions. For

the moment, results have proved to be negative and therefore the existence of axions is an attractive but speculative hypothesis.

The main purpose of the present paper is to show that Asymptotic Giant Branch (AGB) stars can also be used successfully as astroparticle physics laboratories. Since they are very bright, their photometric and spectroscopic properties are well known; for example, the AGB luminosity function can be used to test the efficiency of any phenomenon which is related with the production, removal or transport of energy. Furthermore, the possibility of observing directly the ongoing nucleosynthesis provides a rare opportunity to obtain information about the internal physical conditions. We recall that AGB stars are formed by a dense and degenerate core made up of carbon and oxygen (the CO core) surrounded by two interacting burning shells. The typical densities and temperatures of the CO core and of the He and H-rich layers make these stars a suitable environment to check the reliability of the theory of nuclear and particle physics.

In order to illustrate the possible use of AGB stars in the framework of astroparticle research, we will address the question of the existence of axions (Peccei and Quinn 1977a and 1977b). There are two types of axion models, the hadronic model or KSVZ (Kim 1979, Shifman et al. 1980) and the DFSZ (Zhitniskii 1980, Dine et al. 1981) model. In the first model, the axion couples to hadrons and photons and in the second one also to charged leptons. The axion mass is $m_{ax} = 0.62 \text{ eV} (10^7 \text{ GeV}/f_a)$, where f_a is the Peccei–Quinn scale and the axion coupling to matter is proportional

to f_a^{-1} . In principle, the model does not put any constraint on the value of f_a , so the limits to the m_{ax} must be obtained from experimental arguments.

Within the accepted mass range of DFSZ axions, 10^{-5} eV $\leq m_{\text{ax}} \leq 0.01$ eV (see Raffelt, 1998), axions produced in stellar interiors can freely escape from the star and remove energy, as do neutrinos. The possibility of using stellar interiors to constraint the axion mass was early recognised (Fukugita et al. 1982). The axion energy loss rates depend on the axion coupling strenght to electrons, photons and nucleons and the corresponding coupling constants depend on the axion mass and other model dependent constants. In this way axion mass limits are obtained.

Axions may couple to electrons (Kim 1987; Cheng 1988; Raffelt 1990; Turner 1990 and Kolb and Turner 1990); the axionic fine structure constant is taken as $\alpha = g^2/4\pi$, g is a dimensionless coupling constant that in the DFSZ models is $g = 2.83 \times 10^{-8} m_a / \cos^2\beta$, m_a is the axion mass in meV (10^{-3} eV) and $\cos^2\beta$ is a model-dependent parameter that is usually set equal to 1.

In models in which axions couple to electrons, the two most interesting types of axion interaction that can occur in stellar interiors are photoaxions ($\gamma + e \rightarrow e + a$), which is a particular branch of the Compton scattering, and bremsstrahlung axions ($e + [Z, A] \rightarrow [Z, A] + e + a$) (see Raffelt, 1990). Figure 1 illustrates the axion energy loss rates for these two kinds of interactions, for two chemical compositions. Compton emission strongly increases with temperature (approximately as T^6) and is almost independent of the density. It is, however, inhibited by electron degeneracy. Thus, Compton emission is important in non-degenerate He-burning regions, when the temperature and, in turn, the photon density are high enough. Bremsstrahlung requires greater densities and is not damped at large electron degeneracies. Thus, it is dominant in degenerate He and CO cores.

As yet, few works have included axion interactions in stellar model computations (see Raffelt 1996 and references therein). Isern, Hernanz & García-Berro (1992) use the rate of change of the pulsational period of the white dwarfs during the cooling sequence to constrain the axion mass. Such a rate depends on the cooling rate, namely: $dt/d\ln P \propto dt/d\ln T$, where P is the period of pulsation and T is the temperature of the white dwarf. If the white dwarf has not entered the crystallizing region of the cooling sequence, the discrepancy between the rate of change of the period due to photons alone, which can be obtained from models, and the observed one, which can be assumed to be caused by photons and axions, is

$$\frac{L_{\text{phot}} + L_{\text{ax}}}{L_{\text{phot}}} = \frac{\dot{P}_{\text{obs}}}{\dot{P}_{\text{mod}}}$$

In such a way, Isern, Hernanz & García-Berro (1992 and 1993) found, assuming $\cos^2\beta = 1$, that $m_{\text{ax}} \lesssim 8.7, 15$ and 12 meV by using the seismological data of the white dwarfs G117–B15A, L19–2 and R548, respectively.

Other constraints can be obtained from the possible influence of axions on the evolution of low mass red giants. These stars develop a degenerate He core in which axions, if they exist, could produce a significant energy loss. Dearborn, Schramm and Steigman (1986) found that the helium ignition would be suppressed for values of m_{ax} over a certain

limit. Unfortunately they overestimated the energy loss rate and later on, Raffelt and Dearborn (1987) found that, with the current limits, He ignition would never be suppressed. These authors derived the most stringent limit at that time, for the axion-photon coupling, from the duration of the helium burning lifetime, $m_{\text{ax}} \lesssim 0.7$ eV (KSVZ model). Raffelt and Weiss (1995) subsequently reexamined the problem, analyzing the effects of the axion-electron coupling in observable quantities, such as the luminosity of the RGB (red giant branch) tip. They concluded that m_{ax} is lower than 9 meV, assuming $\cos^2\beta=1$ (DFSZ model). Another limit was obtained for the coupling strenght to photons by Raffelt (1996) by comparing the number of HB (horizontal branch) with the number of RGB stars of galactic Globular Clusters, giving $m_{\text{ax}} \lesssim 0.4$ eV (DFSZ model). The most stringent limit come from the SN 1987A, constraints on the axion-nucleon coupling (Janka et al. 1996; Keil et al. 1997) give, taken into account the overall uncertainties, $m_{\text{ax}} \lesssim 0.01$ eV for both, KSVZ and DFSZ models (Raffelt, 1998).

If axions exist, this would be of major consequence on the evolution of AGB stars. In fact, in both the He shell and in the CO core the physical conditions for an important emission of axions are met. Inside the core there are no nuclear reactions and the gain of gravitational energy would be balanced by neutrino and axion energy losses. The He-burning shell reaches temperatures above 3×10^8 K, much higher than those experienced during the central He-burning, and this could induce a huge production of photoaxions. Therefore axions could alter the stellar lifetime and change the final mass of the CO core.

In the following sections we will present various models of low and intermediate mass stars in the range of masses $0.8 \leq M/M_{\odot} \leq 9$, with and without axion interactions. In particular we assume three different values of the leading parameter m_{ax} (the axion mass), namely: 0, 8.5 and 20 meV (in the following Case 0, 1 and 2 respectively) and set always $\cos^2\beta=1$. Note that the larger value is roughly double the maximum value proposed by Raffelt (1998) yet still marginally compatible with the properties of white dwarfs. We show that the inclusion of axions would imply a significant modification of the AGB characteristics. We do not address the question of setting an astrophysical upper limit of the axion mass here, since this requires a profound comparison between observations of galactic and Magellanic Clouds AGB stars and will be done in a forthcoming paper.

2 THE MODELS

We have followed the evolution of a set of low and intermediate mass stars ($M=0.8, 1.5, 3, 5, 7, 8$ and $9 M_{\odot}$) with solar metallicities, $Z=0.02$ and $Y=0.28$. This mass interval includes stars that ignite He in degenerate conditions (0.8 and $1.5 M_{\odot}$), stars that ignite He in non-degenerate conditions but form a degenerate CO core ($3-7 M_{\odot}$) and go through the entire AGB phase, and stars that ignite C in partially degenerate conditions (8 and $9 M_{\odot}$). The evolutionary sequences are started at the ZAMS phase. For the two smaller masses (0.8 and $1.5 M_{\odot}$) we stopped the sequence at the onset of the He flash. All the other sequences were terminated at the beginning of the thermal pulse phase or at C ignition. Due to the large amount of computer time required to compute

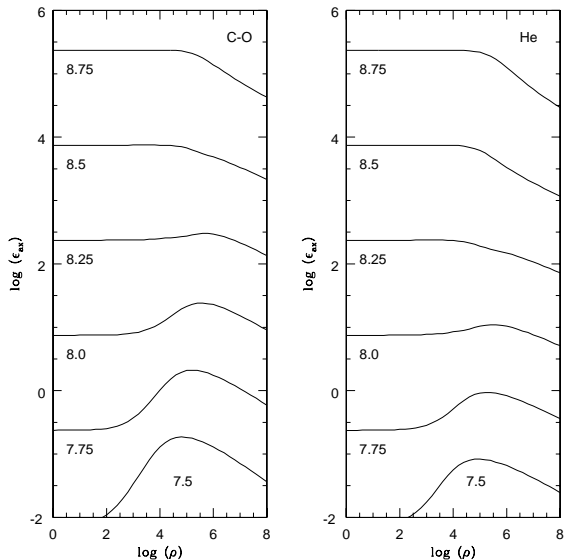


Figure 1. Axion energy loss rate (erg/g/s) as a function of the density (g/cm^3) for different temperatures ($\log(T)$ are indicated) and 2 compositions, pure He and a mixture of C and O (50% each). The mass of the axion is assumed to be 8.5 meV.

thermally pulsing models, only the $5 M_{\odot}$ sequences (with and without axions) were followed throughout this phase.

All the evolutionary sequences of stars were computed with the FRANEC code (Frascati RApson Newton Evolutionary Code), as described by Chieffi and Straniero (1989). The most recent updates of the input physics were described by Straniero, Chieffi and Limongi (1997). When included, the axion energy loss rate have been computed according to Raffelt and Weiss (1995) in the case of Bremsstrahlung in degenerate conditions and Compton and according to Raffelt (1990) in the case of Bremsstrahlung in non degenerate conditions.

Finally, for the $5 M_{\odot}$ star, we considered the case in which only the CO core experiences axion energy losses, in order to distinguish the relative effects on the core and on the He shell and between the AGB and HB phases.

3 APPROACHING THE AGB

Table 1 summarizes the results of the computed evolutionary sequences. From column 1 to 10 we report: the total mass (in solar units), the axion mass (in meV), the surface He mass fraction after the first dredge-up, the tip luminosity of the first RGB (red giant branch), the mass of the He core at the beginning of the He-burning (in solar units), the central He burning life time, the He core mass (in solar units) at the end of central He burning, the E-AGB (early asymptotic giant branch) life time, the surface He mass fraction after the second dredge-up and the CO core mass (in solar units) at the end of the E-AGB.

During the central H-burning and up to the base of the RGB, the energy loss due to axions is negligible. However, when the temperature in the degenerate He core of a low mass star approaches 10^8 K, the contribution of the axion

interactions to the energy balance becomes significant. In spite of the different initial chemical composition, our results for the $0.8 M_{\odot}$ star are in good agreement with those of Raffelt and Weiss (1995). This is no surprise since our axion rates are mainly taken from them. For instance, they obtained an increment of the mass of the He core at the onset of the He-flash of $0.022 M_{\odot}$ and $0.056 M_{\odot}$ for $m_{ax} = 8.9$ and 17.9 meV respectively, while we obtain $0.021 M_{\odot}$ and 0.065 for axion masses of 8.5 and 20 meV respectively.

Note that some widely used expressions like *delay to higher densities* or *He ignition is delayed* might be misleading. The He ignition does indeed occur when the central density is higher, but the density at the off centre ignition point in our calculations is lower (namely 30–40 % less in Case 2 than in Case 0). This point is situated further from the centre in those models that include axions, since the maximum temperature moves outwards as a consequence of the strong axion cooling in the central region. For example, in the case of a $1.5 M_{\odot}$ star, the ignition occurs at $0.14 M_{\odot}$, $0.25 M_{\odot}$ and $0.40 M_{\odot}$ in Cases 0, 1 and 2 respectively. Similar differences are obtained in the $0.8 M_{\odot}$. Furthermore, He ignition is not *delayed* in time, but *anticipated*. The reason is that axion emission accelerates the contraction of the He core. For instance, concerning the $0.8 M_{\odot}$, the RGB evolutionary time is about 150 Myr ($\sim 6\%$) lower in Case 2 than in Case 0, while that of $1.5 M_{\odot}$ is 68 Myr ($\sim 10\%$) lower. The luminosity at the RGB tip (column 4) is also increased (a factor ~ 2 in Case 2) by axions in those stars that ignite He in a degenerate core.

The evolution of the more massive models ($M \geq 3 M_{\odot}$) is not affected by axions until the central He-burning is well established. As already found in low mass stars by Raffelt and Dearborn (1987), since the nuclear burning must supply the energy lost by axions, the temperature is higher and He consumption is faster. The reduction of the total evolutionary time of the He-burning phase (column 6) varies from nearly 40% for the $3 M_{\odot}$ to 6% for the $9 M_{\odot}$ (for the higher value of the axion mass, Case 2). In the models in which the smaller axion mass value was used, the reduction is obviously less: 11% for the $3 M_{\odot}$ and negligible for the $9 M_{\odot}$. Owing to the contraction of the evolutionary time, the H-burning shell has less time to advance in mass and so the final He core mass is reduced (column 7 in Table 1). As a consequence of the higher temperature in the He-burning core, the 3α reaction is favoured with respect to the concurrent α -burning of ^{12}C . Thus at the end of the He-burning, the abundance of carbon is greater. For instance, in the $5 M_{\odot}$ model, the central C abundance changes from 0.224 in Case 0 to 0.322 in Case 2. On the whole, the larger the stellar mass the smaller the effect of axion emission.

4 THE AGB

The Asymptotic Giant Branch is characterized by two different phases, namely the Early AGB (E-AGB) and the thermal pulse phase (TP-AGB). During the E-AGB, the H and the He-burning shells are simultaneously active. However fuel consumption is faster in the inner He-burning shell and so the mass separation between the two burning regions becomes progressively smaller. The advancing He-burning induces an expansion and a cooling of the more external lay-

Table 1. Properties of the models during the HB and E-AGB phases

M_T	M_{ax}	He_s^1	$\log L_{tip}$	M_{He}^1	Δt_{He}	M_{He}^2	Δt_{E-AGB}	He_s^2	M_{CO}
0.8	0.0	0.298	3.451	0.479
	8.5	0.298	3.559	0.501
	20.	0.299	3.750	0.544
1.5	0.0	0.294	3.445	0.477
	8.5	0.294	3.561	0.500
	20.	0.295	3.765	0.547
3.0	0.0	0.296	2.560	0.378	141	0.545	9.2	0.296	0.549
	8.5	0.296	2.587	0.378	127	0.530	6.6	0.296	0.524
	20.	0.298	2.707	0.378	85.6	0.479	5.0	0.298	0.459
5.0	0.0	0.296	3.186	0.654	20.8	1.024	1.20	0.324	0.856
	8.5	0.296	3.187	0.651	20.0	1.014	0.75	0.340	0.744
	20.	0.297	3.192	0.648	16.6	0.968	0.51	0.347	0.645
7.0	0.0	0.296	3.685	1.001	7.3	1.591	0.39	0.366	1.005
	8.5	0.298	3.686	1.001	7.05	1.579	0.240	0.377	0.881
	20.	0.299	3.688	1.001	6.2	1.537	0.115	0.381	0.787
8.0	0.0	0.300	3.881	1.201	5.1	1.882	C-ignition
	8.5	0.300	3.882	1.201	5.1	1.889	C-ignition
	20.	0.301	3.883	1.201	4.64	1.585	C-ignition
9.0	0.0	0.301	4.052	1.422	4.1	2.217	C-ignition
	8.5	0.301	4.053	1.422	4.1	2.209	C-ignition
	20.	0.302	4.055	1.422	3.9	2.165	C-ignition

ers. If the stellar mass is large enough, the H-burning shell is finally quenched. In such a case, the convective envelope can penetrate the H/He discontinuity, bringing to the surface the products of the H-burning (basically N and He). This is called the second dredge-up and marks the end of the E-AGB and the beginning of the thermal pulses. During this second part of the AGB phase, the H-burning shell is reignited while the He-burning one is quenched. Once a suitable amount of He is accumulated by the H-burning, a strong He-burning starts again, expands the external layer and again quenches the H burning. In a very short time the He consumption has progressed such that the He shell again extinguished, the contraction takes place and H is reignited. This sequence repeats until the mass loss removes the envelope and the star leaves the AGB. Note that during the pulse the region between the two shells becomes convectively unstable and fully mixed. After the thermal pulse, when quiescent He-burning occurs and the H-burning shell is still extinguished, a new convective envelope penetration at the H/He discontinuity brings to the surface the products of the He burning (essentially carbon) and that of the neutron capture nucleosynthesis (s-process, see e.g. Straniero et al. 1996, Gallino et al. 1998). This is the so-called third dredge-up. The following sections describe the modifications to this scenario induced by axion emission.

4.1 The early-AGB and the second dredge-up

The most important effect of axion emission during the E-AGB is the faster consumption of fuel within the He-shell. This causes the H-shell to be extinguished more quickly and the second dredge-up to occur earlier, resulting in a markedly smaller CO core mass. This behaviour is shown in Figure 2.

The reduction of the duration of the E-AGB phase (column 8, Table 1) is in the range of 30–40%, for Case 1; and as much as 50–70% for Case 2. The CO core mass at the end of the E-AGB is reported in column 10. Note the significant differences with respect to the standard case. For the $7M_{\odot}$ model, the CO core mass obtained for the highest axion mass is even smaller than that obtained for the standard $5M_{\odot}$. This reduction is not equal for all the masses, varying from 5% to 15% in Case 1, and from 15% to 28% in Case 2 for stars in the mass range $3M_{\odot}$ to $7M_{\odot}$.

As a consequence of the deeper penetration of the convective envelope, the surface He abundance after the 2^{nd} dredge-up is greater (see column 9 in Table 1). For example, for the $5M_{\odot}$ stars, the H/He discontinuity moves inward $0.17M_{\odot}$ in Case 0, and $0.30M_{\odot}$ in Case 2.

As expected, the temperature within the CO core is lowered by the larger energy loss. Figure 3 clearly illustrates such an occurrence.

In order to elucidate how far these changes of the E-AGB phase are due to the previously altered evolution (central He-burning) and/or to axion emission in the He shell, we have limited their inclusion to the CO core. The result

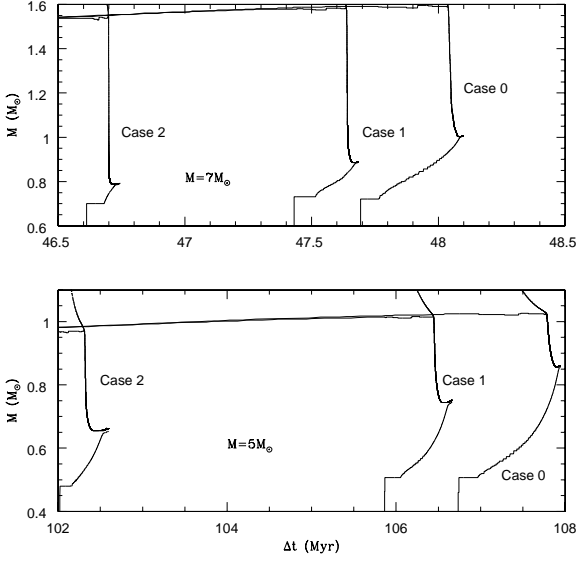


Figure 2. Evolution with time of the C-O/He discontinuity, He/H discontinuity and the inner border (in mass coordinates) of the convective envelope for Case 0: $m_{ax}=0.0$, Case 1: 8.5 and Case 2: 20 meV. Upper panel: $7M_{\odot}$. Lower panel: $5M_{\odot}$.

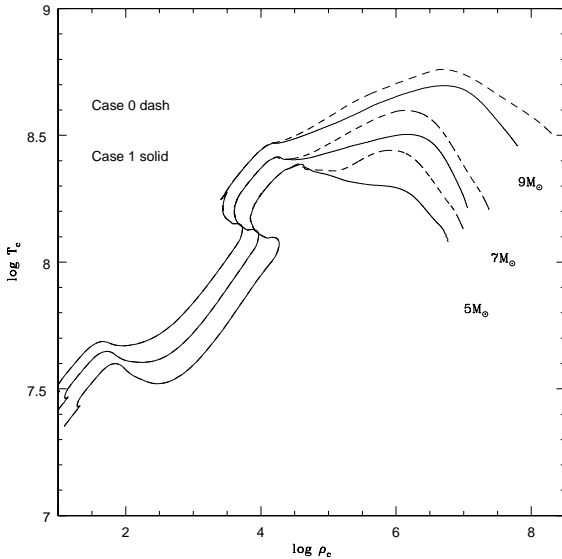


Figure 3. Central temperature as a function of the central density for the masses $9M_{\odot}$, $7M_{\odot}$ and $5M_{\odot}$. Case 0: $m_{ax}=0$ meV; Case 1: $m_{ax}=8.5$ meV.

is that the duration of the E-AGB is similar to the one obtained in the case of the full axion inclusion. This result is important, since it clearly shows the strong influence of the physical conditions in the degenerate core on the evolution of the active shells. Furthermore, it means that the effects found during the E-AGB are almost independent of the axion energy losses during the previous phases.

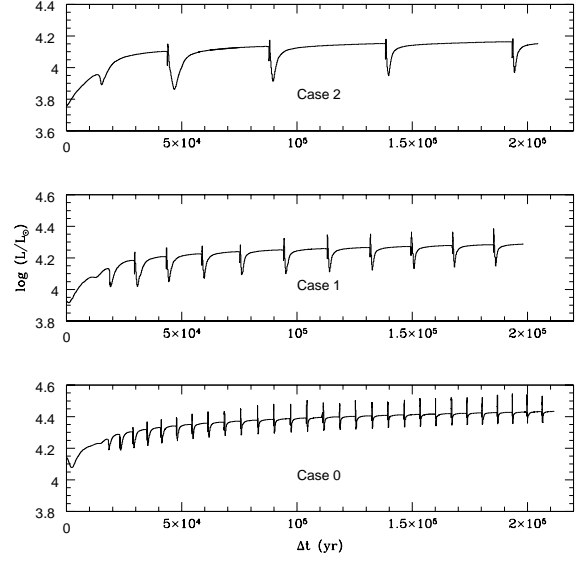


Figure 4. Evolution with time of the surface luminosity during the TP-AGB phase for the $5M_{\odot}$ star. Lower panel: $m_{ax}=0.0$ (Case 0); Middle panel: $m_{ax}=8.5$ meV (Case 1); Upper panel: $m_{ax}=20$ meV (Case 2).

4.2 The thermal pulse phase

During the TP phase, axion emission in the core and in the He-burning shell becomes more important. In Table 2 we report some properties of the three sequences computed for the $5M_{\odot}$, namely the He core mass at the beginning of the TP (column 1), the duration of the interpulse period (column 2), the increment of the He core mass during the interpulse (column 3), the penetration (in solar masses) of the convective envelope at the time of the 3rd dredge-up (column 4) and the λ parameter, i.e. the ratio between the quantities in columns 3 and 4 (column 5). In figure 4 we show the evolution of the surface luminosity. The evolution of the location of the external boundary of the CO core, of the He core and that of the internal boundary of the convective envelope are shown in figure 5.

The most striking consequence of axion emission is the extension of the evolutionary time. The duration of a typical interpulse period increases by a factor of ~ 2.5 in Case 1 and by a factor of ~ 6 in Case 2, both with respect to the standard case. This is due to the combined effects of the lower core mass (see the previous subsection) and the axion cooling of the He shell. The luminosity is about 1.5 times greater in Case 0 than in Case 2. However, note that all three sequences asymptotically follows the classical core mass/luminosity relation (Paczynsky 1977; Iben and Renzini, 1983). This is shown in figure 6 for Case 0 and 1. The temperature at the bottom of the convective envelope (figure 7) is lower in models which include axion emission. Thus the occurrence of hot bottom burning in the more advanced AGB evolution and the consequent deviation from the core mass/luminosity relation (Blöcker and Schönberner 1991) should be reduced by this axion cooling.

More He is accumulated by the H-burning during the extended interpulse period, so that more nuclear energy

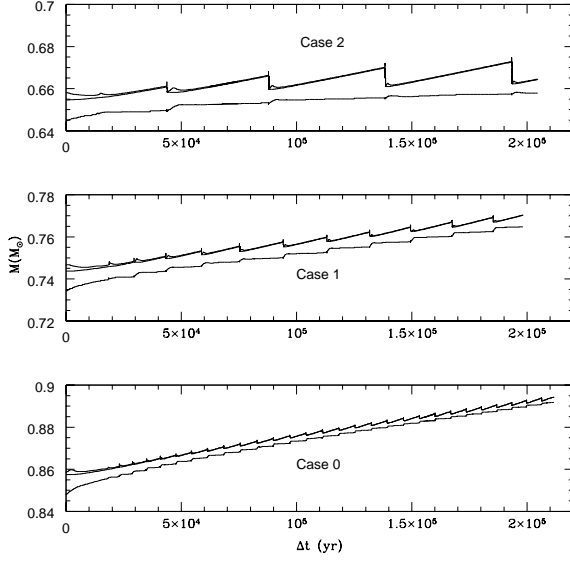


Figure 5. Evolution with time of the C-O/He discontinuity, H/He discontinuity and the inner border (in mass coordinates) of the convective envelope at the TP-AGB phase, for the $5M_{\odot}$ star. Lower panel: $m_{ax}=0.0$ (Case 0); Middle panel: $m_{ax}=8.5$ meV (Case 1); Upper panel: $m_{ax}=20$ meV (Case 2).

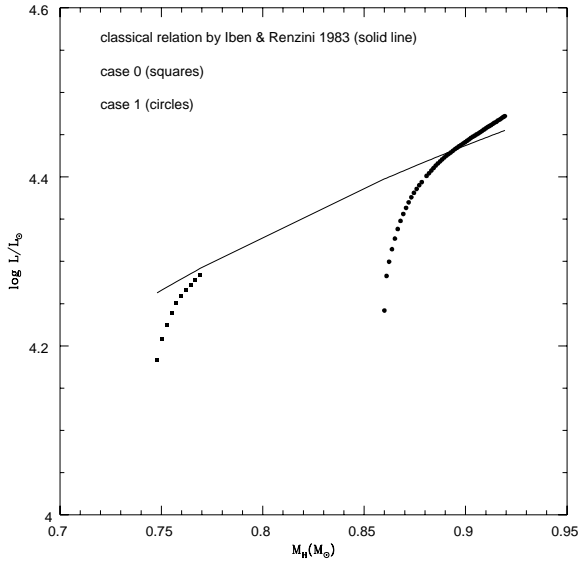


Figure 6. Core Mass-Luminosity Relation for AGB stars. Continuous line (IR83): computed following Iben-Renzini (1983); Case 0: the $5M_{\odot}$ star with $m_{ax}=0.0$ and Case 1: same mass with $m_{ax}=8.5$ meV

must be produced in the pulse in order to expand the stored matter. A stronger thermal pulse favours the following dredge-up. For this reason the third dredge-up starts after the first TP in the two sequences including axions, while in Case 0 it starts after the 4th TP. The mass of He and C material mixed in the envelope is nearly twice as much in Case 1 and ~ 8 times larger in Case 2, both with respect to Case 0.

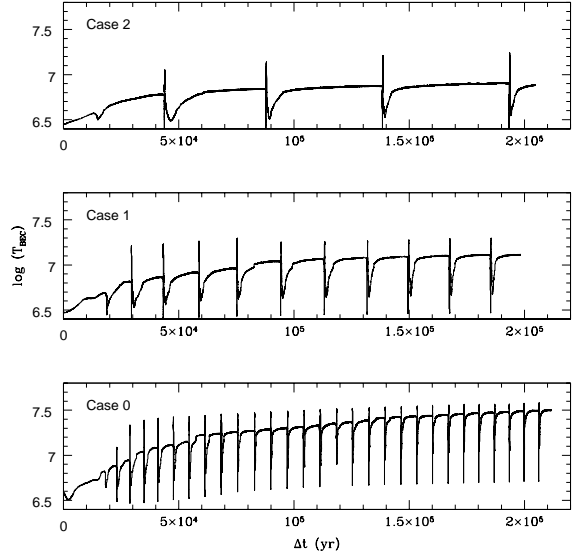


Figure 7. Evolution with time of the temperature at the bottom of the convective envelope at the TP-AGB phase, for the $5M_{\odot}$ star. Lower panel: $m_{ax}=0.0$ (Case 0); Middle panel: $m_{ax}=8.5$ meV (Case 1); Upper panel: $m_{ax}=20$ meV (Case 2).

With a resolution of just $1M_{\odot}$, the minimum mass for which carbon ignition occurs before the TP-AGB phase, i.e. M_{up} , is the same in all three cases, namely $\sim 8 M_{\odot}$. However the C ignition occurs farther from the centre in models with axions. For instance, in Case 1 we found an off centre C ignition at $0.93M_{\odot}$ instead of the $0.40M_{\odot}$ in the standard case. Note that the mass of the CO core is smaller when axions are included, namely $1.148 M_{\odot}$ instead of $1.259 M_{\odot}$.

Finally, it is interesting to note that the inclusion of axions modifies the initial/final mass relation (see e.g. Weidemann 1987). During the thermal pulses, the mass of the CO core increases as a result of the accretion of C freshly synthesized by the He flashes. However, the observed luminosity of AGB stars (Weidemann 1987; Wood et al. 1992) and the observed mass-loss rate at this phase, indicate that the occurrence of too many pulses is prevented by the removal of the envelope (Bedijn 1987, Baud and Habing 1983, van der Veen, Habing and Geballe 1989). The mass of the CO white dwarf is essentially determined by the value reached at the end of the E-AGB phase (see Vassiliadis and Wood 1993; Blöcker 1995). In figure 8 we compare the CO core mass (a guess for the WD mass) with the initial mass (progenitor mass), for Case 0 and Case 1. Two more masses have been included, 4 and $6 M_{\odot}$.

The relative abundance of white dwarfs with masses m_0 and m_1 is given by

$$r(m_1, m_0) = \frac{\delta n(m_1)}{\delta n(m_0)} = \left[\frac{M(m_0)}{M(m_1)} \right]^{\alpha} \frac{(dM/dm)_{m_0}}{(dM/dm)_{m_1}}$$

where we have assumed that the star formation rate per unit volume in the solar neighbourhood is constant and that the initial mass function follows Salpeter's law with $\alpha = 2.35$ and $M(m)$ is the relationship between the mass of the parent star and that of the white dwarf. Note that if it were possible to separate the influence of the mass loss and the influence of

Table 2. Properties of the $5M_{\odot}$ model during the TP-AGB phase

M_H	Δt_{ip}	ΔM_H	ΔM_{D-up}	λ
Case 2: 20 meV				
0.661	2.50E-03	...
0.666	4.49E+04	7.80E-03	6.50E-03	0.83
0.670	4.96E+04	1.03E-02	8.80E-03	0.85
0.673	5.68E+04	1.17E-02	1.02E-02	0.87
Case 1: 8.5 meV				
0.748
0.750	1.37E+04	2.40E-03	0.50E-03	0.21
0.753	1.54E+04	3.10E-03	1.30E-03	0.42
0.755	1.66E+04	3.60E-03	1.70E-03	0.47
0.757	1.89E+04	3.90E-03	2.00E-03	0.51
0.760	1.88E+04	4.20E-03	1.90E-03	0.45
0.762	1.85E+04	4.20E-03	1.80E-03	0.43
0.765	1.82E+04	3.90E-03	1.70E-03	0.44
0.767	1.78E+04	4.10E-03	2.00E-03	0.49
0.769	1.77E+04	4.20E-03	1.80E-03	0.43
Case 0: 0 meV				
0.860
0.861	4.84E+03	1.03E-03
0.862	5.70E+03	1.24E-03
0.864	6.10E+03	1.30E-03	1.33E-04	0.10
0.865	6.34E+03	1.57E-03	3.26E-04	0.21
0.867	6.60E+03	1.72E-03	4.80E-04	0.28
0.868	6.80E+03	1.85E-03	5.56E-04	0.30
0.869	6.93E+03	1.93E-03	6.61E-04	0.34
0.871	7.05E+03	2.02E-03	7.99E-04	0.40
0.872	7.12E+03	2.10E-03	8.60E-04	0.41
0.873	7.16E+03	2.14E-03	8.75E-04	0.41
0.875	7.16E+03	2.17E-03	8.85E-04	0.41
0.876	7.14E+03	2.20E-03	9.94E-04	0.45
0.877	7.13E+03	2.23E-03	9.06E-04	0.41
0.878	7.07E+03	2.22E-03	1.00E-03	0.45
0.881	7.00E+03	2.29E-03	1.07E-03	0.47
0.882	6.99E+03	2.28E-03	1.17E-03	0.51
0.883	6.97E+03	2.30E-03	1.22E-03	0.53
0.884	6.95E+03	2.32E-03	1.24E-03	0.53
0.885	6.90E+03	2.32E-03	1.21E-03	0.52
0.886	6.84E+03	2.31E-03	1.25E-03	0.54
0.887	6.80E+03	2.32E-03	1.26E-03	0.54
0.888	6.73E+03	2.31E-03	1.28E-03	0.55
0.889	6.70E+03	2.32E-03	1.29E-03	0.56
0.891	6.66E+03	2.32E-03	1.23E-03	0.53
0.892	6.56E+03	2.29E-03	1.17E-03	0.51
0.893	6.45E+03	2.25E-03	1.19E-03	0.53
0.894	6.41E+03	2.25E-03	1.28E-03	0.57

axions during the AGB phase, it would be possible to obtain very strong constraints to the properties of these particles.

5 CONCLUSIONS

We have studied the effects of including axions (DFSZ model) in the evolution of intermediate and low mass stars ($0.8 \leq M/M_{\odot} \leq 9$). Among the various evolutionary phases affected by axion emission, the AGB seems to be the most

promising in terms of obtaining stringent constraints to the theory of particle physics. These effects are:

- 1.- A severe reduction in the size of the final CO core, as compared with the values obtained from standard evolutions, implies some interesting modifications of observable quantities, such as the luminosity of AGB stars and their residual mass. Concerning the AGB luminosity function in particular, the axion emission would imply a deficit of bright AGB stars. The initial/final mass relation is also substan-

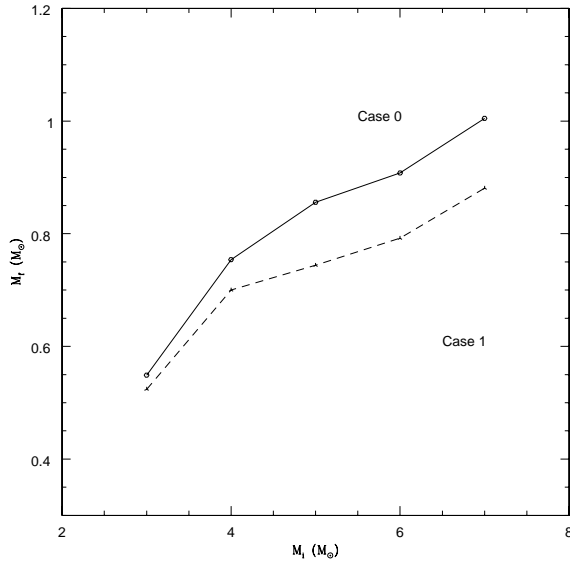


Figure 8. Final and Initial masses; solid line= Case 0 ($m_{ax}=0.0$) and dashed line= Case 1 ($m_{ax}=8.5$ meV).

tially modified and a deficit of massive white dwarfs is expected.

2.- As a consequence of the axion cooling, the convective instabilities that characterize the double nuclear shell burning are more extended and the chemical composition of the surface could be significantly modified. A stronger 3^rd dredge-up implies that the C star stage could be more easily (and perhaps rapidly) obtained. In addition the surface abundance of s-elements, which are the products of the neutron capture nucleosynthesis occurring during the interpulse (through the $^{13}C(\alpha, n)$ neutron source) and during the thermal pulse (through the $^{22}N(\alpha, n)$), are other important "observable" quantities to be used to constrain the properties of the axions as well as those of any other weak interactive particle proposed in non-standard theories of particle physics.

It is a great pleasure to thank Alessandro Chieffi and Marco Limongi for helpful discussion. This work has been supported in part by the DGICYT grants PB96-1428 and ESP98-1348, by the Italian Minister of University, Research and Technology (Stellar Evolution project), by the Junta de Andalucía FQM-108 project and by the CIRIT(GRC/PIC).

REFERENCES

- Avignone III F.T. et al. 1997 Phys. Lett. B (submitted)
 Baud B. Habing H.J. 1983, AA, 127, 73
 Bedijn P.J. 1987, AA, 186, 136
 Blöcker T. Schönberner D. 1991, AA 244, L43
 Blöcker T. 1995, AA 297, 727
 Burrows A., Turner M.S. Brinkmann R.P. 1990, Phys. Rev. D 39 1020
 Cheng Y. 1988, Phys. Rep. 158, 1
 Chieffi A. Straniero O. 1989, ApJSS, 71, 47
 Chieffi A. Straniero O. Salaris M. 1995, ApJ, 445, L39
 Dine M. Fischler W. Srednick M. 1981, Phys. Lett. B104, 199

- Dearborn D. Schramm D.N. Steigman G. 1986, Phys. Rev. Lett. 56, 26
 Domínguez I. Chieffi A. Limongi M. Straniero O. 1998, submitted to ApJ
 Faulkner J. Gilliland R.N. 1985, ApJ, 229, 994
 Fukugita M. Watamura S. Yoshimura M. 1982, Phys. Rev. D26, 1840
 Gallino R. Arlandini C. Busso M. Lugaro M. Travaglio C. Straniero O. Chieffi A. Limongi M. 1998, ApJ 497, 388
 Gattone A.O. 1999, Nucl. Phys. Proc. Suppl. 70, 59
 Haggmann C. et al. 1996, Nucl. Phys. (Proc. Suppl.) B51, 209
 Haggmann C. et al. 1998, Phys. Rev. Lett. 80, 2043
 Iben I. Renzini A. 1983, ARAA, 21, 271
 Isern J. Hernanz M. Garcia-Berro E. 1992, ApJ, 392, L23
 Isern J. Hernanz M. Garcia-Berro E. 1993, NATO-ASI Series, White Dwarfs: Advances in Observation and Theory, Ed. M. Barstow, Kluwer Academic Publisher, 139
 Janka H.T. Keil W. Raffelt G. D. Seckel 1996, Phys. Rev. Lett. 76, 2621
 Keil W. et al. 1997, Phys. Rev. D56, 2419
 Kim J.E. 1979, Phys. Rev. Lett. 43, 103
 Kolb E.W. Turner M.S. 1990, The Early Universe, Ed. Addison Wesley
 Lazarus D.M. et al. 1992, Phys. Rev. Lett. 69 2333
 Matsuki S. et al. 1996, Nucl. Phys. B51, 213
 Moriyama S. 1998, Search for Solar Axions by Using Strong Magnetic Field and X ray Detectors, Ph.D. Thesis, University of Tokyo
 Moriyama S. Minowa M. Namba T. Inoue Y. Takasu Y. Yamamoto Y. 1998, Phys. Lett. B434, 147
 Nakagawa M. Adachi T. Kohyama Y. Itoh N. 1988, ApJ, 326, 241
 Paczynski, B. 1970 Acta. Astron. 20, 47.
 Peccei R.D. Quinn H. 1977a, Phys. Rev. Lett. 38, 1440
 Peccei R.D. Quinn H. 1977b, Phys. Rev. D 16, 1791
 Press W.H. Spergel D.N. 1985, ApJ, 296, 679
 Raffelt G.C. Dearborn D. 1987, Phys. Rev. D 36, 2211
 Raffelt G.C. 1990, Phys. Rep. 198, 1
 Raffelt G.C. Weiss A. 1995, Phys. Rev. D51, 1495
 Raffelt G.C. 1996, Stars as Laboratories for Fundamental Physics, Ed. University of Chicago Press, Chicago.
 Raffelt G.C. 1998, in Beyond the Desert, Ed. W. Hillebrandt and E. Muller, MPA-P
 Shifman M. Vainshtein A. Zakharov V. 1980, Nucl. Phys. B166, 493
 Sikivie P. 1983 Phys. Rev. Lett. 51, 1415
 Steigman G. Sarazin C.L. Quintana H. Faulkner J. 1978 AJ 83 1050
 Straniero O. Chieffi A. Limongi M. Busso M. Gallino R. Arlandini C. 1997, ApJ 478, 332
 Turner M.S. 1990, Phys. Rep. 197, 67
 van Bibber K. et al. 1994, Int. J. Mod. Phys. Suppl. D 3, 33
 van der Veen W. Habing H.J. Geballe T. 1989, A&A, 226, 108
 Vassiliadis, E. Wood P.R. 1993, ApJ, 413, 641
 Weidemann V., Koester D. 1983, AA, 121, 77
 Wood P.R., Whiteoak J.B., Hughes S.M.G., Bessel M.S., Gardner F.F., Hyland A.R. 1992, ApJ, 397, 552
 Zhitnitskii, A.P. 1980, Sov. J. Nucl. Phys. 31, 260
 Zioutas K. et al 1998, submitted to Nucl. Instrum. Meth. A.